

# GQD/Bi<sub>2</sub>O<sub>3</sub> Composite for high-efficient photocatalysts

Chengli Tang<sup>1</sup>, Limei Zhang<sup>2</sup>

<sup>1</sup>Chongqing Chemical Industry Vocational College, Chongqing, 401220, PR China

<sup>2</sup>School of Chemistry and Chemical Engineering, Chongqing University, Chongqing, 40004, PR China

**Abstract:** Bismuth oxide (Bi<sub>2</sub>O<sub>3</sub>) is one of the potential visible-light photocatalytic materials, however, due to low electron mobility and short minority carrier diffusion length, the photocatalytic activity of Bi<sub>2</sub>O<sub>3</sub> is restricted. The GQD/Bi<sub>2</sub>O<sub>3</sub> composites were synthesized stably depositing single-crystalline graphene quantum dots (GQDs) with absorption edge at ~10nm, prepared by using a top-down method. The GQD-Bi<sub>2</sub>O<sub>3</sub> heterojunctions were successfully established, the photo-generated electrons transfer from the Bi<sub>2</sub>O<sub>3</sub> to the GQDs at the interface of the GQD-Bi<sub>2</sub>O<sub>3</sub> heterojunctions, result in efficient electron-hole pairs separation and higher photocatalytic efficiency. The optimum visible performance is achieved at GQD content of 1.0 wt %, the RhB dye was nearly completely decoloured after 90 min of visible-light irradiation, and then decrease at higher doping levels due to the thicker GQD layer will cover the active sites of Bi<sub>2</sub>O<sub>3</sub>, thus leading to the greatly reduced catalytic activity.

## 1 Introduction

The degradation of organic pollutants by using semiconductor photocatalysts has been extensively studied during the past years because of its advantages of high efficiency, energy conservation and no secondary pollution[1-3]. Bismuth oxide (Bi<sub>2</sub>O<sub>3</sub>), a semiconductor that has a narrow bandgap of 2.8 eV, has recently received considerable attentions as potential visible-light photocatalytic materials [4-5]. However, Bi<sub>2</sub>O<sub>3</sub> alone exhibits a poor photocatalytic activity primarily because its conduction band is too low for the oxidation of the surface O<sub>2</sub> to O<sup>-</sup>, leading to a high recombination rate of the electron hole pairs [6-7]. To improve the photocatalytic activity of Bi<sub>2</sub>O<sub>3</sub>, several strategies have been attempted in the literatures, e.g. element doping, surface modification with noble metal, coupling with other semiconductors or quantum dots (QDs) like CdS, GaAs, CdTe, ZnS, etc. [8-10]. In this paper, GQDs/Bi<sub>2</sub>O<sub>3</sub> nanocomposite was successfully synthesized by a facile and green method, and its photocatalytic performance for degrading Rhodamine B (RhB) with different GQD contents was evaluated under visible-light irradiation.

## 2 Materials and Methods

### 2.1.Reagents and chemicals

All the reagents were of analytical grade and used without further purification. Water-soluble graphene oxide (GO) sheets were prepared from natural graphite powders by using a hydrothermal method. Graphene sheets (GSs) were obtained by the thermal deoxidization of GO sheets in a tube furnace at 200-300°C for 2 h with a heating rate

of 5 °C·min<sup>-1</sup> in a nitrogen atmosphere.

### 2.2.Preparation of Bi<sub>2</sub>O<sub>3</sub> nanoparticles

Bi<sub>2</sub>O<sub>3</sub> nano-particles were prepared by using a facile solvothermal method. 0.364 g of Bi(NO<sub>3</sub>)<sub>3</sub>·5H<sub>2</sub>O and 0.6 g of Polyvinylpyrrolidone (PVP) were dissolved into a 55 mL ethylene glycol solution of nitric acid (1 M). The mixture was continuously stirred for 0.5 h, and then transferred to a Teflon-lined stainless-steel autoclave (100 mL). The solvothermal treatment was conducted at 433 K for 12 h. Afterwards, the mixture was cooled to room temperature and then separated by centrifugation, the resulted solid was washed three times by using deionized (DI) water and absolute ethanol, dried at 333 K for 12 h and calcined at 543 K for 3 h in air to obtain the final product.

### 2.3.Preparation of GQDs

In a typical procedure to prepare GQDs, 0.1 g of GSs were oxidized in a mixture of concentrated H<sub>2</sub>SO<sub>4</sub> (10 ml) and HNO<sub>3</sub> (30 ml) for 24 h under ultrasonication. The mixture was then diluted with DI water (250 ml) and filtered through a 0.22 μm microporous membrane to remove the acids. Then the pH value of the mixture was adjusted to 8 by using NaOH and transferred to a Teflon-lined autoclave (50ml) and heated at 200 °C for 10 h. After being cooled to room temperature, the resulting black suspension was filtered through a 0.22 μm microporous membrane. The obtained colloidal solution was further dialyzed in a dialysis bag (molecular weight cut off = 3500 Da) overnight to give the strongly fluorescent GQDs.

## 2.4.Synthesis of GQDs/Bi<sub>2</sub>O<sub>3</sub>Composites

The composites were prepared by using a hydrothermal deposition method. Typically, Bi<sub>2</sub>O<sub>3</sub> (0.1g) was added to 10 mL of GQD solution under stirring for 1h at room temperature to obtain a homogeneous suspension. Afterwards, the suspension was transferred into a Teflon-lined autoclave (20 ml), heated at 150 °C for 4 h and dried in a vacuum oven at 80 °C overnight to obtain the GQDs/Bi<sub>2</sub>O<sub>3</sub> composites containing 1.0 wt% of GQDs.

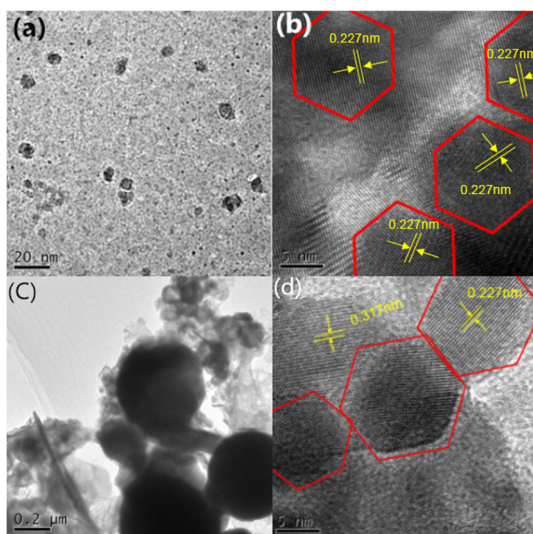
## 2.5.Photocatalytic Test

The degradation of Rhodamine B (RhB) was evaluated by adding 0.01 g of the prepared GQDs/Bi<sub>2</sub>O<sub>3</sub> photocatalysts in 100 ml of RhB solution (10 mg·L<sup>-1</sup>) at room temperature. The visible light was obtained from a 350W xenon lamp equipped with a 420 nm ultraviolet cutoff filter.

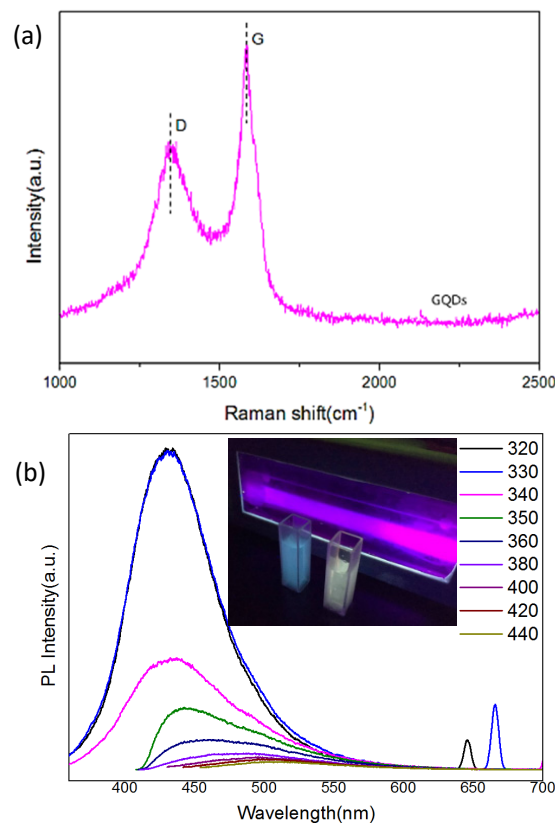
## 2.6.Characterization.

TEM observations were performed on a JEOL JEM-2010F electron microscope operating at 200 kV. Fourier transform infrared spectroscopy (FT-IR) spectra were performed on Thermo Nicolet Avatar 370 FT-IR.

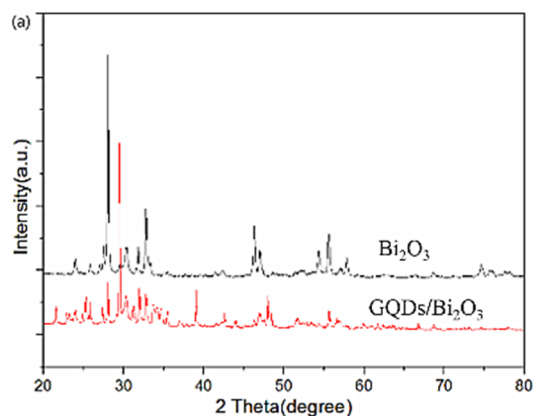
## 3 Results and Discussion



**Fig. 1.** TEM and HRTEM images of GQDs (a, b) and 1.0 wt % doping GQDs/ Bi<sub>2</sub>O<sub>3</sub> composites (c, d)



**Fig. 2.** Raman (a) and PL (b) spectrum of GQDs  
 TEM images in Fig. 1a shows that the prepared GQDs have a relatively uniform particle distribution with an average lateral size of 10nm. As displayed in the HRTEM images (Fig.1b), an obvious single-crystal structure is observed for the GQDs, with an interplanar spacing of 0.227 nm. Moreover, the successful synthesis of GQDs was also verified by the Raman and PL analysis. The two characteristic D and G bands at 1355 cm<sup>-1</sup> and 1580 cm<sup>-1</sup>, which are attributed, respectively, to disordered carbon and ordered sp<sup>2</sup> carbon, can be clearly observed in the Raman spectrum (Fig. 2a). The PL spectra for the aqueous suspension of GQDs (Fig. 2b) shows the typical excitation-dependent PL behaviors, exhibiting blue color (inset in Fig. 2b) when being excited at 325 nm.



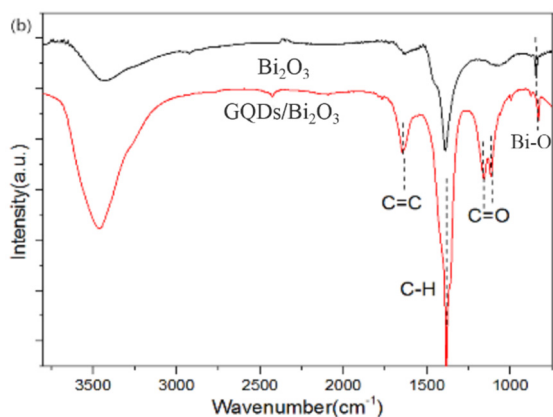


**Fig. 3.** XRD (a) and FT-IR (b) spectrum of  $\text{Bi}_2\text{O}_3$  alone and 1.0 wt % GQDs/ $\text{Bi}_2\text{O}_3$  composite.

Under the hydrothermal “sintering” conditions, GQDs were stably deposited on the surface of  $\text{Bi}_2\text{O}_3$  nanoparticles. TEM and HRTEM images (Fig.1c and 1d) of the GQDs/ $\text{Bi}_2\text{O}_3$  composites with 1.0 wt% GQD loading demonstrate that GQDs are well dispersed on  $\text{Bi}_2\text{O}_3$  nanoparticles. The structure of the GQDs/ $\text{Bi}_2\text{O}_3$  composites is further characterized by using the XRD, FT-IR. As shown in Fig.3a, the XRD patterns of both  $\text{Bi}_2\text{O}_3$  and GQDs/ $\text{Bi}_2\text{O}_3$  exhibit the typical diffraction of anatase  $\text{Bi}_2\text{O}_3$  [JCPDS: 41-1449]; while the interaction between GQDs and  $\text{Bi}_2\text{O}_3$  during the hydrothermal process leads to the shift of the diffraction peaks to the higher angles in the XRD pattern of the GQDs/ $\text{Bi}_2\text{O}_3$  composites. Compared with that of  $\text{Bi}_2\text{O}_3$ , the characteristic peaks attributed to C=C vibration at 1647  $\text{cm}^{-1}$ , C-H vibration at 1384  $\text{cm}^{-1}$ , C=O vibration at 1160  $\text{cm}^{-1}$ , and C-O vibration at 1116  $\text{cm}^{-1}$  are observed in the IR spectrum of the GQDs/ $\text{Bi}_2\text{O}_3$  composites (Fig.3b), confirming the existence of GQDs in the composites.

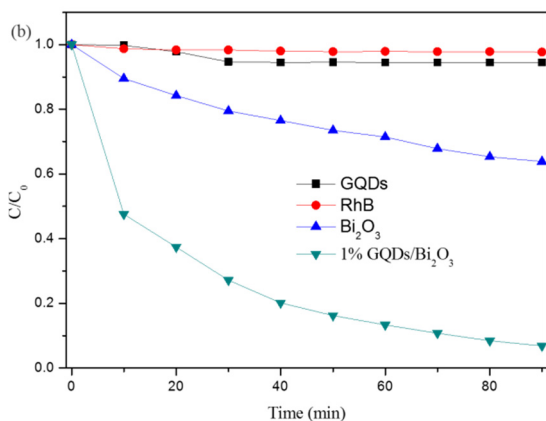
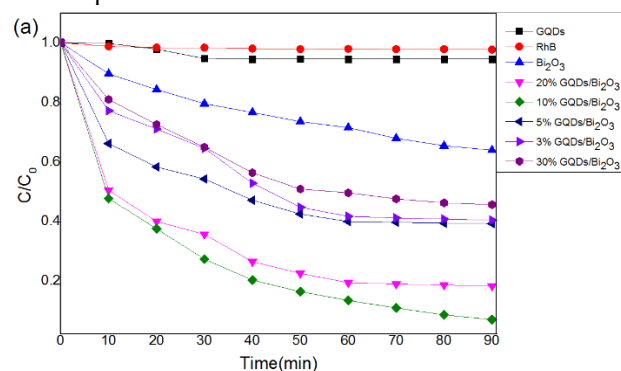


**Fig.4.**(a) Photocatalytic degradation rate curves of RhB using GQDs/ $\text{Bi}_2\text{O}_3$  composites with different contents of GQDs as catalysts under the visible light . (b)Photocatalytic degradation rate curves of RhB using GQD,  $\text{Bi}_2\text{O}_3$ , and GQDs/ $\text{Bi}_2\text{O}_3$  as photocatalysts under the visible light.

Fig.4 shows that the photocatalytic activity of the composites to degrade RhB are significantly enhanced by coupling GQDs with  $\text{Bi}_2\text{O}_3$ . By using the GQDs/ $\text{Bi}_2\text{O}_3$  composites with the optimum GQD loading of 1 wt%, 91% RhB can be decoloured after 90 min of visible-light irradiation. For comparison, by using the same amount of pure  $\text{Bi}_2\text{O}_3$  or GQDs as the photocatalysts, only 28% or 6% RhB can be degraded within the same irradiation time (Fig. 4b). As expected, the visible-light response of pure  $\text{Bi}_2\text{O}_3$  is limited by its nature of wide-band gap and high recombination rate of the electron hole pairs. The poor catalytic performance of pure GQDs can be ascribed to the large exciton binding energy ( $\sim 0.8$  eV estimated for 2 nm GQDs) that greatly increases the recombination rate of photoexcited electrons and holes. It also can be observed from Fig.4a that the optimum GQD loading for the composites as the photocatalysts is 1 wt%, a further increase in the GQD loading beyond the optimum value will cause a significant decrease of the photocatalytic activity of the composites.

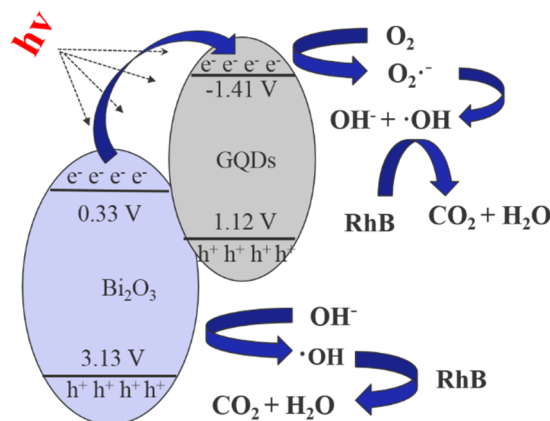


**Fig. 5.** Schematic of GQDs/ $\text{Bi}_2\text{O}_3$ nanocomposites combined with the possible reaction mechanism of photocatalytic procedure under Visible-Light Irradiation.

The photocatalytic mechanism of the GQDs/ $\text{Bi}_2\text{O}_3$  composites can be lustrated in Fig.5. Under the irradiation of visible light, electrons can be excited from the VB to the CB in both GQDs and  $\text{Bi}_2\text{O}_3$ . Electrons in the CB of GQDs and holes in the VB of  $\text{Bi}_2\text{O}_3$  could combine with  $\text{O}_2$  and  $\text{OH}^-$  in the solution, respectively, to form  $\cdot\text{OH}$ , which is the most important reactive specie to degrade RhB. The coupling of  $\text{Bi}_2\text{O}_3$  and GQDs in the composites leads to the transfer of the photo-generated electrons from  $\text{Bi}_2\text{O}_3$  to GQDs, which rest at the GQD- $\text{Bi}_2\text{O}_3$  interface, resulting in the efficient electron-hole pairs separation and higher photocatalytic efficiency. When the GQD loading in the composite is too high, a thicker GQD layer will cover the active sites of  $\text{Bi}_2\text{O}_3$ , thus leading to the greatly reduced catalytic activity. Therefore, for the design of GQD-based hybrid photocatalysts with superior visible-light catalytic performance, it is crucial importance to construct monodispersed nanoparticle heterojunctions. We postulate that a monodispersion and thin monolayer of

soluble GQDs can be deposited on the surface of Bi<sub>2</sub>O<sub>3</sub> nanoparticles by a hydrothermal process, and thus the optimum GQD-Bi<sub>2</sub>O<sub>3</sub> heterojunctions at the nanoscale can be established at the low loading level.

Thus, the heterojunction material has alluring visible-light response, we can make a conclusion: on the one hand, the bandgap of GQDs is tuned as lowly as possible for harvesting more solar light, on the other hand, allow for construction of GQD-Bi<sub>2</sub>O<sub>3</sub> heterojunctions at the interface of the two materials to drive the electron transfer between the GQDs and Bi<sub>2</sub>O<sub>3</sub>.

## 4 Conclusions

In summary, water-soluble GQDs are successfully loaded onto the Bi<sub>2</sub>O<sub>3</sub> in optimum density to form novel GQD sensitized Bi<sub>2</sub>O<sub>3</sub> heterojunctions. The incorporation of GQDs can sensitize Bi<sub>2</sub>O<sub>3</sub> and inhibit the fast recombination effectively, the photocatalytic activities under visible light irradiation obviously increased than pure Bi<sub>2</sub>O<sub>3</sub>. The optimum visible performance could be achieved when containing 1.0 wt % of GQD content, where the RhB dye was almost completely decolorated after 90 min of visible-light irradiation. However, the catalytic activity of Bi<sub>2</sub>O<sub>3</sub> would decrease when increasing the GQD content, since thicker GQD layer could cover the active sites of Bi<sub>2</sub>O<sub>3</sub>.

## Acknowledgments

This work was supported by the Foundation of Chongqing Chemical Industry Vocational College (Grand No. HY2019-KJRC01).

## Reference

1. Singaram B, Varadharajan K, Jeyaram J, Rajendran R, Jayavel V. (2017) Preparation of cerium and sulfur codoped TiO<sub>2</sub> nanoparticles based photocatalytic activity with enhanced visible light[J]. *J Photoch Photobio A.*, 349: 91-99.
2. Hongbo Fu CP, Wenqing Yao, Yongfa Zhu. (2005) Visible-Light-Induced Degradation of Rhodamine B by Nanosized Bi<sub>2</sub>WO<sub>6</sub>[J]. *The Journal of Physical Chemistry B.*, 109: 22432-22439.
3. Chen C, Ma W, Zhao J. (2010) Semiconductor-mediated photodegradation of pollutants under visible-light irradiation[J]. *Chemical Society reviews.*, 39: 4206-4219.
4. Zhang X, Li L, Wen S, Luo H, Yang C. (2017) Design and synthesis of multistructured three-dimensionally ordered macroporous composite bismuth oxide/zirconia: Photocatalytic degradation and hydrogen production[J]. *Journal of colloid and interface science.*, 499: 159-169.
5. Maruthamani D, Vadivel S, Kumaravel M, Saravanakumar B, Paul B, Dhar SS, et al. (2017) Fine cutting edge shaped Bi<sub>2</sub>O<sub>3</sub> rods/reduced graphene oxide (RGO) composite for supercapacitor and visible-light photocatalytic applications[J]. *Journal of colloid and interface science.*, 498: 449-459.
6. Jiang H-Y, Liu G, Li P, Hao D, Meng X, Wang T, et al. (2014) Nanorod-like  $\alpha$ -Bi<sub>2</sub>O<sub>3</sub>: a highly active photocatalyst synthesized using g-C<sub>3</sub>N<sub>4</sub> as a template[J]. *RSC Adv.*, 4: 55062-55066.
7. Sun W, Zhang H, Lin J. (2014) Surface Modification of Bi<sub>2</sub>O<sub>3</sub> with Fe(III) Clusters toward Efficient Photocatalysis in a Broader Visible Light Region: Implications of the Interfacial Charge Transfer[J]. *The Journal of Physical Chemistry C.*, 118: 17626-17632.
8. Tada H, Fujishima M, Kobayashi H. (2011) Photodeposition of metal sulfide quantum dots on titanium(IV) dioxide and the applications to solar energy conversion[J]. *Chemical Society reviews.*, 40: 4232-4243.
9. Xie Y, Ali G, Yoo SH, Cho SO. (2010) Sonication-assisted synthesis of CdS quantum-dot-sensitized TiO<sub>2</sub> nanotube arrays with enhanced photoelectrochemical and photocatalytic activity[J]. *ACS applied materials & interfaces.*, 2: 2910-2914.
10. Xiao FX, Miao J, Liu B. (2014) Layer-by-layer self-assembly of CdS quantum dots/graphene nanosheets hybrid films for photoelectrochemical and photocatalytic applications[J]. *J Am Chem Soc.*, 136: 1559-1569.